NENE
International Conference
Nuclear Energy for New Europe

Direct Contact Condensation Induced Water Hammer Simulation Using Computational Fluid Dynamics Code

MD Arman Arefin[1,2], Ivo Kljenak[1,3]

[1]University of Ljubljana
Faculty of Mathematics and Physics
Jadranska ulica 19
SI-1000 Ljubljana, Slovenia

[2]LUT University
LUT School of Energy Systems
Yliopistonkatu 34,
FI-53850 Lappeenranta, Finland

[3]Jozef Stefan Institute
Reactor Engineering Division
Jamova cesta 39
SI-1000 Ljubljana, Slovenia

MD.Arman.Arefin@student.lut.fi, ivo.kljenak@ijs.si

ABSTRACT

Direct contact condensation (DCC) induced water hammer in a horizontal pipe was simulated on the local instantaneous scale, using a Computational Fluid Dynamics code with a modification introduced via a user-defined function. The model was first validated using an experiment from the literature. The model was then applied to a DCC-induced water hammer in a T-junction. Conditions were modified to infer the behaviour of the pressure spike. Results suggest that setting the inlet water liquid temperature close to the outlet one and increasing the liquid water mass flow rate will significantly reduce the pressure spike.

1 INTRODUCTION

Water hammer occurs if a pressure surge, or a high-pressure shockwave, propagates through a piping system when a fluid in motion is forced to change direction or stop abruptly. This may also occur due to direct contact condensation (DCC), resulting from the interaction of steam and subcooled liquid water. DCC-induced water hammer is a likely phenomenon during accidental events in light water nuclear reactors, and could cause significant damage to the piping.

The combination of the very short time scale on which DCC occurs and the random shape of the gas-liquid interface (in the sense that it cannot be predetermined exactly) on which condensation occurs results in an (aleatory) uncertainty of the magnitude of the pressure surge. This means that experimental values of maximum pressure may vary significantly from one test to the next, even if initial and boundary conditions are kept constant. First, this makes it difficult to replicate theoretically experimental values of maximum pressures. Second, such results of theoretical simulations will always be uncertain (with regard to real phenomena), regardless of the sophistication of the modelling.

In the present paper, DCC-induced water hammer was simulated on the local instantaneous scale, with the application of Large Eddy Simulation. The Computational Fluid Dynamics (CFD) code ANSYS Fluent was used, with a modification introduced via a user-defined function (UDF). The model was first validated using an experiment from the literature. Then, the model was applied to DCC-induced water hammer in a T-junction. After the simulation results were compared with results from a similar case in the literature, the model was used to study the influence of liquid water subcooling and mass flow rate on the magnitude of the pressure spike.

2 THEORETICAL MODELLING

The direct condensation induced water hammer was simulated with a two-phase flow model using the volume of fluid numerical method and Large Eddy Simulation turbulent model, implemented in the ANSYS Fluent code. The generic features of the modelling are not described here, but only some specific modifications implemented via a UDF.

For the saturation temperature, the user can upload a table of temperature *vs* pressure. However, in the case of water hammer, the fluctuations of pressure are too high with sudden drops and rises, so the Fluent code will cause floating point exception errors and the simulation will stop. The UDF was thus implemented to calculate the saturation temperature with the fluctuations of pressure by solving the following equation:

$$T_{sat} = \frac{237.3\, ln(\frac{P_{vap}+101325}{611})}{17.27 - ln\left(\frac{P_{vap}+101325}{611}\right)} + 273 \tag{1}$$

where P_{vap} is the vapor pressure of the species in the vapor phase. This equation can capture the rapid temperature changes and therefore replicate the eventual mass transfer (condensation). That is, if the vapor temperature is lower than the saturation temperature, the mass transfer rate is calculated, based on the temperature difference between the saturation temperature and the liquid water temperature. Otherwise, no mass transfer occurs.

Some other equations are also implemented in the UDF to calculate the turbulent length scale, the turbulent velocity scale and the liquid water heat transfer coefficient, among other matters.

3 SIMULATIONS

3.1 Model validation

For the validation of the proposed model, the experiment shown in Fig. 1 was considered, as described by Štrubelj et al. [1,2]. The experiment was performed in the PMK-2 test facility of the Hungarian Atomic Energy Research Institute KFKI. At one end of a horizontal pipe, water vapor (steam) was injected. After the tube was filled with vapor, subcooled liquid water was injected at the other end. The experiment was simulated with a two-dimensional model.

The experimental temperatures at four locations in the tube (at distances 258 mm, 851 mm, 1452 mm and 2003 mm from the liquid water inlet, respectively, and referred as T1, T2, T3, and T4) are shown in Fig. 2. Corresponding simulation results from ref. [1], as well as those obtained by the model used in the present work, are shown in Fig. 3. Although the lower temperatures obtained with the proposed model are not so distinct from each other as the experimental results, they are still in the same range. At time 20 s, the temperatures in the experiment for positions T1 and T4 are between 320 K and 380 K, whereas in the simulation with the proposed model, they are between 340 K and 375 K. Therefore, the calculated mean absolute error of temperature is around 13 K. Although this agreement is by no means a proof of the model accuracy, it is still sensible enough for the model to be used for further studies.

3.2 Computational model for T-junction

In the present paper, DCC-induced water hammer was studied in a fictional T-junction. The geometry of the configuration is shown in Fig. 4. There are two pipes in the junction; the horizontal one (main pipe) has a length of 500 mm and a diameter of 50 mm; the vertical one (branch pipe) has a length of 1000 mm and a diameter of 10 mm. Two points A and B, located respectively 100 mm and 250 mm from the liquid water inlet, are considered for the analysis. A three-dimensional model of the described system was developed.

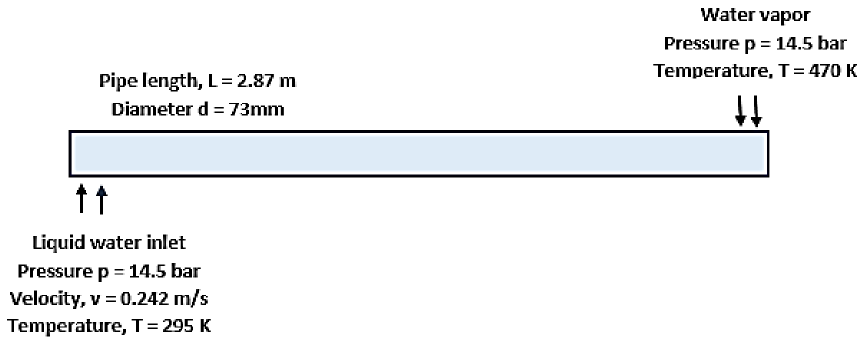

Figure 1. Experimental case (PMK-2 experiment) for model validation [1,2].

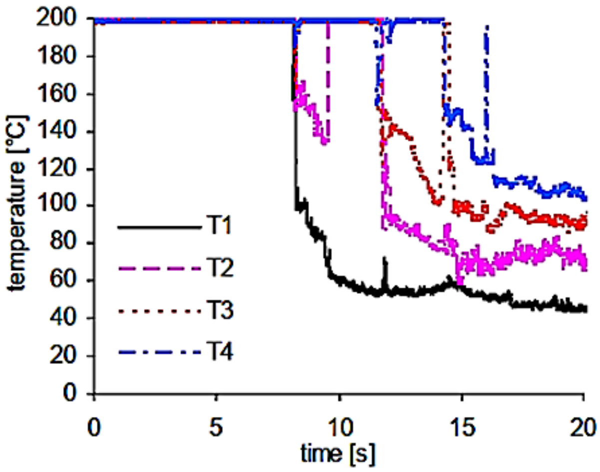

Figure 2. Temperature measurements in PMK-2 experiment.

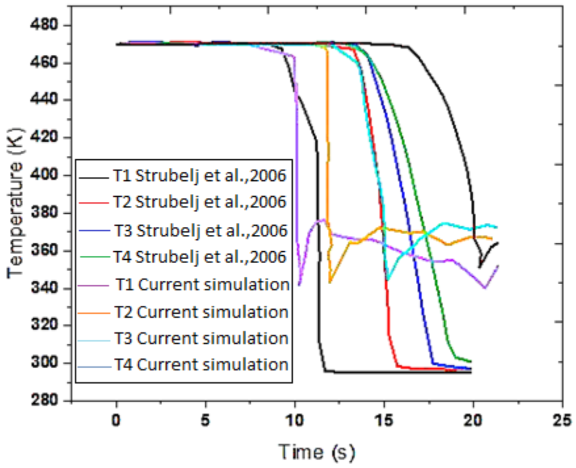

Figure 3. Simulation results (temperature) of PMK-2 experiment.

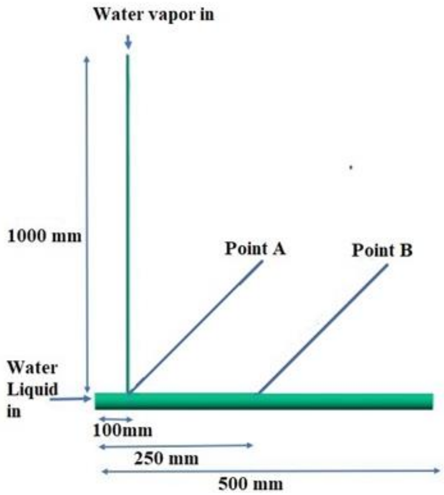

Figure 4. T-junction model for condensation-induced water hammer simulation.

3.3 Simulation set-up

A coupled algorithm was used for pressure-velocity coupling. For the transient, a second-order implicit model was selected. The solution was considered to converge when the residuals were below 10^{-3}. However, for the continuity equation, 10^{-2} was considered as the limit, as it is difficult to converge the continuity equation solution for a coupled modelled unstable flow. The time step was set from the determination of the Courant number, a dimensionless quantity that establishes the relation between the time step and the characteristic time of the transient:

$$C = \frac{\Delta t}{\frac{x_{cell}}{v_{fluid}}} \tag{2}$$

where Δt is the time step size, x_{cell} is the size of cells and v_{fluid} is a characteristic velocity. In principle, the Courant number should be less than 1.0. For the first 10 ms, the time step size was 10^{-6} s, whereas for the rest of the simulation, it was set to 10^{-5} s. Whether the flow is laminar or turbulent is commonly inferred from the Reynolds number. For the steam, the calculated Reynolds number is 4.19×10^{4}, which defines the flow as turbulent. The material properties of liquid water (density, specific heat, thermal conductivity and viscosity) were calculated at the specified temperatures. The boundary conditions are given in Table 1.

Table 1. Boundary conditions

Case	Ambient pressure (MPa)	Steam gauge pressure (Pa)	Steam temperature	Liquid water temperature (K)	Liquid water mass flow (kg/s)	Steam mass flux (kg/m²s)
A	0.1013	0	Saturated	303	0.5	10
B	0.1013	0	Saturated	343	0.5	10
C	0.1013	0	Saturated	363	0.5	10
D	0.1013	0	Saturated	303	5	10

3.4 Analysis of numerical accuracy

The results of a grid independence analysis, performed for the simulation in the T-junction (case A), are shown in Fig. 5. The grid density study was conducted to determine the accuracy and convergence of the simulation. Three different numbers of cells (240319, 303036 and 468530) were taken into account. It is visible that the pressure values are comparable for cell numbers 303036 and 468530, respectively, whereas with the coarsest mesh, the pressure was higher by some 20%. To save computation time while keeping accuracy, the grid with 303036 cells was used for the simulations. The temperature behaviour was not considered here as it is only weakly dependent on the mesh density.

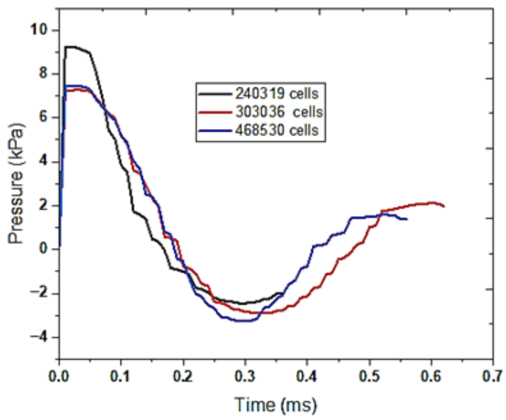

Figure 5. Analysis of numerical accuracy.

4 RESULTS AND DISCUSSION

Unless stated otherwise, the presented results were obtained with the prescribed liquid mass flow rate 0.5 kg/s (Table 1). Figure 6 shows the temperature behaviour at liquid water inlet temperatures of 303 K, 343 K and 363 K, respectively. As may be observed, the temperature is not stable, and repeatedly decreases and increases. These fluctuations are called thermal cycling, which occurs due to the change in temperature in the water vapor and may result in fatigue cracking in pipes. Fluctuations are the result of rapid condensation occurring when cold water is introduced into a pipe filled with water vapor. These temperature fluctuations in the pipe are attributed to the significant transfers of thermal energy as the vapor condenses into liquid due to the liquid water injection. As the water vapor rapidly loses heat and transitions into liquid, it can cause localized temperature changes within the pipe, leading to thermal cycling. These fluctuations of temperature can have several effects, including inducing mechanical stresses on the pipe and potentially causing structural damage. The cycling is more visible at point B than at point A.

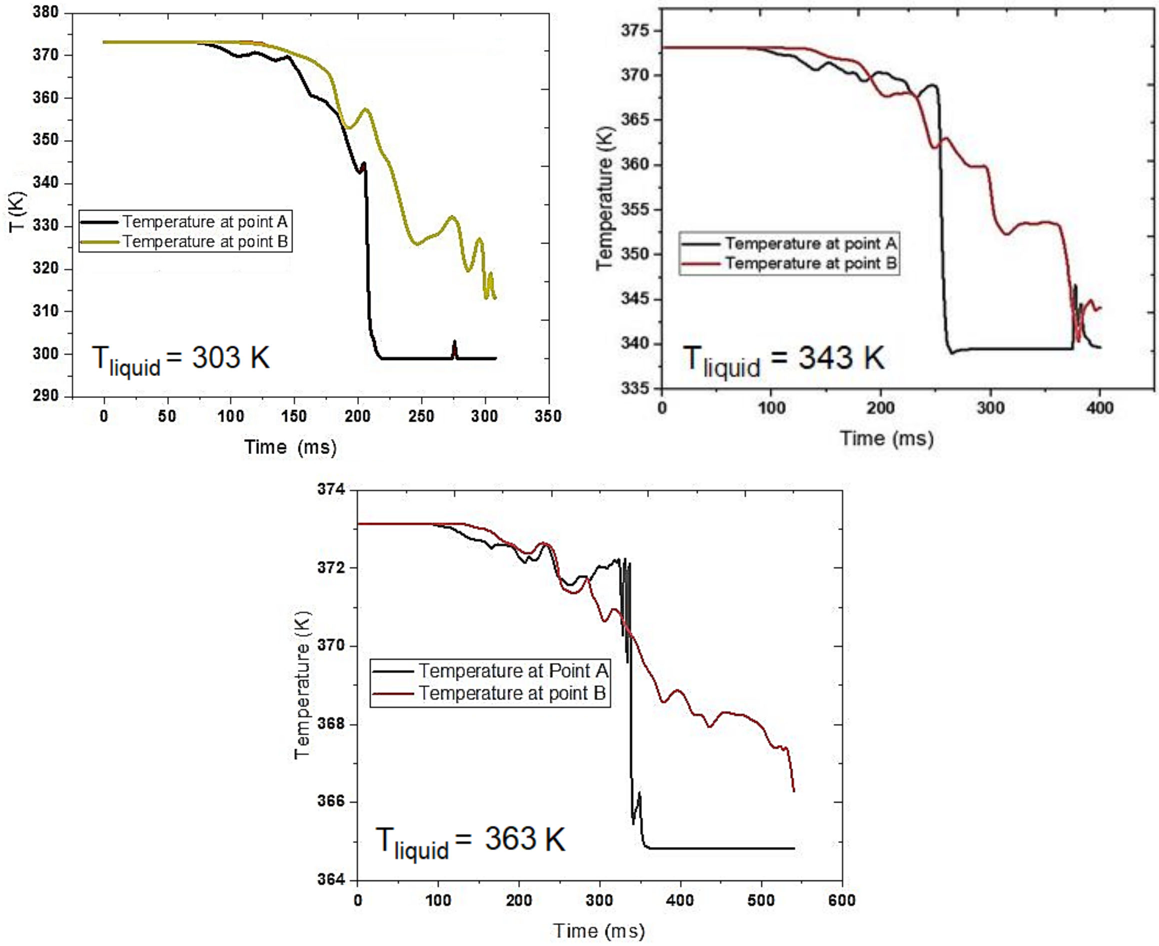

Figure 6. Temperature behaviour at points A and B
at liquid water temperatures 303 K, 343 K and 363 K.

Figure 7 shows the steam volume fraction in the pipe at time 200 ms (just before the water hammer), whereas Fig. 8 shows the corresponding pressure. As one can see, vapor got trapped, so the pressure dropped. What happened next was the sudden rise of the pressure (water hammer) to compensate this pressure drop.

Figure 9 shows the pressure variations with time at point A at liquid water temperatures 303 K, 343 K and 363 K. The results are compared with the results provided by Li et al. [3]. As may be observed, the pressure peaks are higher at low temperature. With the increase of liquid water temperature, the value of the peaks decreases. For a temperature of 303 K, the pressure obtained in the current simulation is higher than in the mentioned reference paper. However, at temperatures of 343 K and 363 K, the results are quite similar. Furthermore, at temperature 363 K, no pressure peaks are visible: with the increase of liquid water temperature, the water hammer reduces (in the sense of pressure increase). The same behaviour was also mentioned by Nariai and Aya [4]. Therefore, the presented novel results are in good agreement with the literature. The probable physical explanation is that with higher liquid water temperature, the condensation rate is lower, thus causing a lower imbalance in the sense of ensuing pressure difference.

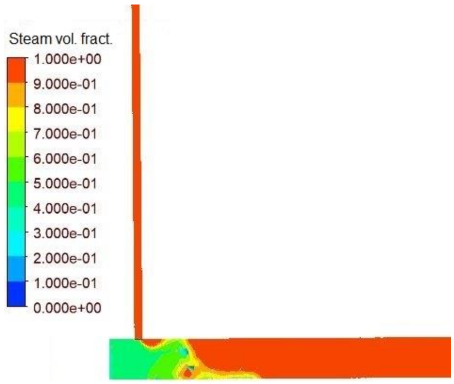

Figure 7. Steam volume fraction at liquid water temperature 303 K (t = 200 ms).

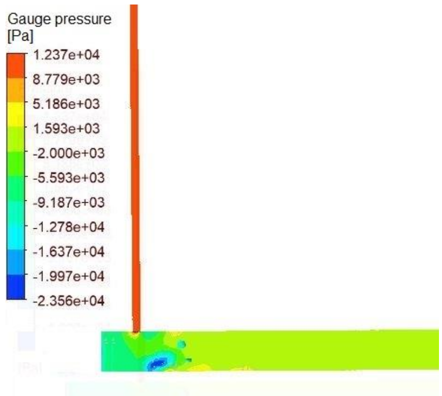

Figure 8. Gauge pressure at liquid water temperature 303 K (t = 200 ms).

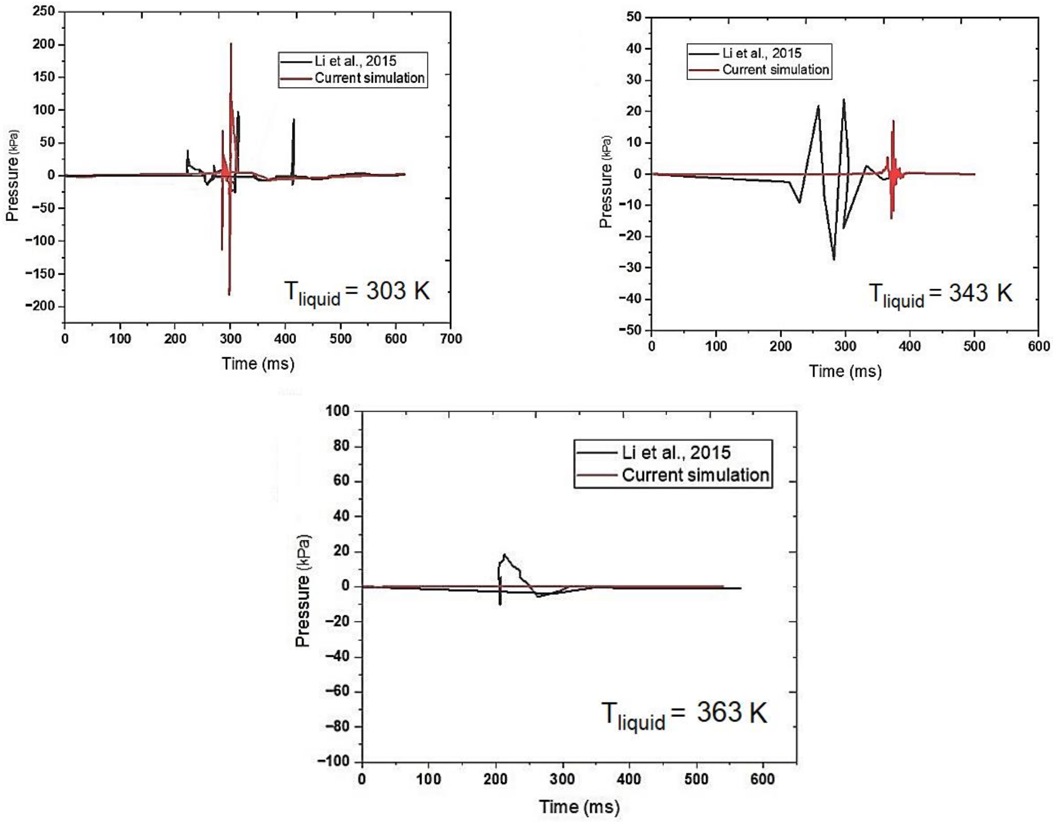

Figure 9. Pressure behaviour at point A at liquid water temperatures 303 K, 343 K and 363 K.

Figure 10 shows the pressure behaviour at point B, again at liquid water temperatures 303 K, 343 K and 363 K. Several pressure peaks are observed at temperature 303 K. The highest peak is about 3.5 kPa, whereas, for temperature 343 K, the peak reduces to 1.5 kPa. Furthermore, at temperature 363 K, no peak is observed. On the occurrence of sudden condensation, the pressure pulses are produced on the steam bubble-like volume which was separated from the upstream steam plume.

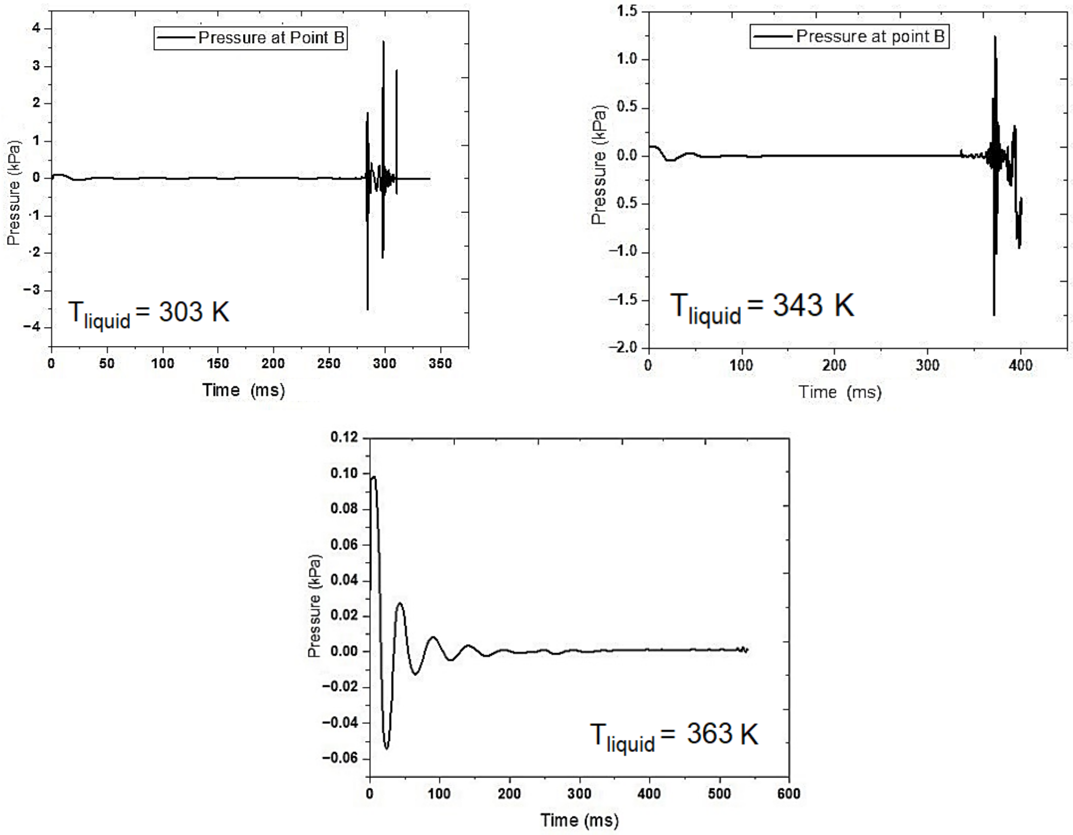

Figure 10. Pressure behaviour at point B at liquid water temperatures 303 K, 343 K and 363 K.

Furthermore, the simulations also revealed that the hammer dampens with the increase of the liquid water mass flow rate. It is thus possible to get rid of the pressure and temperature fluctuations by increasing the mass flow rate of the inlet liquid water. As can be seen from Fig. 9, the pressure peak at 303 K and 0.5 kg/s mass flow rate at point A is around 220 kPa, whereas at the same temperature but a mass flow rate of 5 kg/s the highest peak is around 50 kPa (Fig. 11). Also, at point B, the values are 3.5 kPa and 2.7 kPa at mass flow rates of 0.5 kg/s and 5 kg/s, respectively (Figs. 10 and 11). Furthermore, with the increase of the liquid mass flow rate, the temperature fluctuations also tend to reduce to a certain extent (Fig. 12).

CONCLUSIONS

A model for direct contact condensation induced water hammer, developed by implementing a user defined function in a Computational Fluid Dynamics code, was first validated on experimental results and then used to study the influence of liquid water subcooling and mass flow rate on the magnitude of the pressure spike. The simulations revealed that it is possible to avoid water hammer by increasing the liquid water temperature closer to the saturated steam temperature, and that the water hammer dampens with the increase of the liquid water mass flow rate. This confirms what could also have been expected from physical intuition.

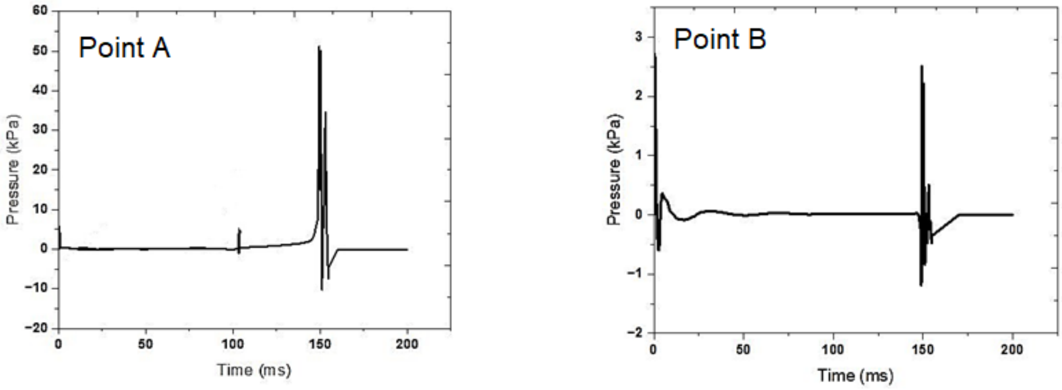

Figure 11. Pressure behaviour at points A and B
(liquid water mass flow rate: 5 kg/s).

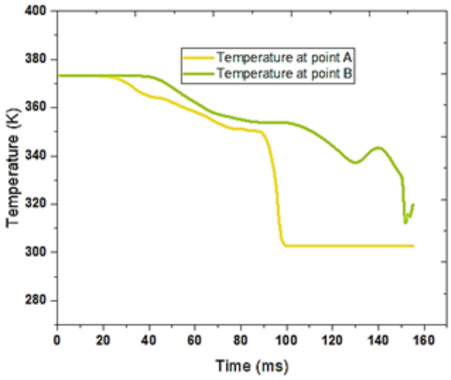

Figure 12. Temperature behaviour at points A and B
(liquid mass flow rate: 5 kg/s).

ACKNOWLEDGMENTS

The authors acknowledge the financial support from the Slovenian Research Agency through grant P2-0026. The contribution of Md Arman Arefin is based on a work within the European Commission SARENA project (2019-2024).

REFERENCES

[1] L. Štrubelj, I. Tiselj, B. Končar, "Modelling of direct contact condensation in horizontally stratified flow with CFX code", Benchmarking of CFD codes for application to nuclear reactor safety, Garching, Germany, 2006.

[2] L. Štrubelj, G. Ézsöl, I. Tiselj, "Direct contact condensation induced transition from stratified to slug flow", Nuclear Engineering and Design 240, 2010, pp. 266–274.

[3] S. Li, P. Wang, T. Lu, "CFD Based Approach for Modeling Steam–Water Direct Contact Condensation in Subcooled Water Flow in a Tee Junction", Progress in Nuclear Energy 85, 2015, pp. 729-746.

[4] H. Nariai, I. Aya, "Fluid and Pressure Oscillations Occuring at Direct Contact Condensation of Steam Flow with Cold Water", Nuclear Engineering and Design 95, 1986, pp. 35-45.